4.4 Modelling of ground acceleration field in the Catania area associated with the Ibleo-Maltese fault system

(A. Zollo and A. Emolo)

4.4.1 *Strong motion simulation*

In this study we simulated the ground motion associated with an earthquake, as large as the one which struck South-Eastern Sicily in 1693, having approximate magnitude M=7 (level I scenario earthquake). We assumed that this event could be associated with the multiple rupture of two near-vertical normal sub-parallel segments dipping NE of the Ibleo-Maltese composite fault system. The parameters which describe the complete source geometry are reported in table 4.3 (Scandone and Meletti, personal written communication).

Table 4.3

	Northern fault segment	**Southern fault segment**
Length	2.25×10^4 m	5.1×10^4 m
Width	1.5×10^4 m	1.5×10^4 m
Top depth	5×10^2 m	5×10^2 m
Strike	352°	346°
Dip	80°	80°
Rake	-90°	-90°
Seismic moment (*)	1.2×10^{19} Nm	2.8×10^{19} Nm
Stress drop (*)	2.5 MPa	2.5 MPa

(*) Values computed by authors

The seismic moments of 1.2×10^{19} Nm and 2.8×10^{19} Nm have been computed respectively for the Northern and Southern fault segments in order to have a total event having magnitude 7, following the moment-magnitude scaling law by Hanks and Kanamori (1979).

To estimate the strong ground motion parameters (PGA and spectral ordinates) we used the mixed statistical-deterministic approach proposed by Zollo *et al.* (1997). The method is based on the massive computation of synthetic accelerograms produced by a large number of possible rupture processes occurring on a given fault (or fault system) whose geometry and mechanism are assumed to be known. Each rupture process is simulated assuming a statistical distribution of kinematic parameters which control the nucleation, the rupture propagation and the space-time slip history during the rupture process.

In the present case, the rupture may nucleate randomly along one of the two fault segments and propagates through the other one once the nearest border has been reached.

Due to the ranges of frequency ($0.5<f<20$ Hz) and distances (near source approximation) considered in our study, we restricted our simulations to the direct S-wave field which largely dominates in amplitude with respect to the other phases when the site effects can be considered weak or negligible. In this case, as explained by Bernard and Madariaga (1984) and Farra *et al.* (1986), for observed wavelenghts shorter than the minimum source-receiver distance, it is possible to consider the asymptotic solution of wave equation as a good approximation of the near source wave field.

The ground acceleration radiated according to the rupture of each fault segment is computed by solving numerically the representation integral (Aki and Richards, 1980).

The space-time slip distribution on the fault is obtained assuming at each point a ramp-like function characterized by three parameters, that is, the rupture time, the rise time and the final slip. Rupture times are computed assuming a uniform rupture velocity on the fault plane while the rise time in chosen equal to the cut-off frequency of the low-pass filter applied on the synthetic accelerograms which corresponds to an instantaneous rise of the slip to its final value at the passage of the rupture front, and to maximizing the amplitude of expected ground motion in the far-field approximation. Under a constant rupture velocity hypotesis, the ω-square behaviour of acceleration spectra can be related to a self-similar slip and stress drop distributions on the fault which follow a negative power law of radial wavenumber. The final slip distribution is then computed by using he k-square model proposed by Herrero and Bernard (1994) and normalizing the obtained slip so as to get the total seismic moment equal to a given value.

In this study we neglected the crustal path effects since we used a homogeneous half-space ($v_S=3.5x10^3$ m/s, $Q_S=300$) because our main interest was to investigate the influence of source complexity on seismic radiation, neglecting complex path phenomena.

As a first order approximation, at a very local scale, the response of a multi-layered structure to a near-vertical incident SH plane wave was computed using the Thomson-Haskell matrix method (Haskell, 1962). The site effects were then modeled by convolution of synthetic accelerograms at a given site by the computed 1D transfer function.

The predictive method proposed by Zollo *et al.* (1997) was recently validated by Emolo and Zollo (1999) who compared the theoretic estimates for the strong motion parameters with the data collected during the main shocks of the 1997 Umbria-Marche seismic sequence.

4.4.2 *Results: spatial variation of peak ground acceleration*

A number of 100 different rupture processes was performed, each of them being characterized by random nucleation point, i.e.randomly occurring on one of the two segments of the Ibleo-Maltese fault system, and different final slip distribution (computed according to the k-square model). The corresponding synthetic accelerograms were computed at each of 44 hypothetical receivers (the black circles in Figure 4.15). We filtered the accelerograms in the 0.5-20 Hz frequency band, choosing the low frequency value in accordance with distances from the fault which are greater than few wavelenghts and the high frequency value in order to cover the useful range for engineering applications.

The peak values are used to generate the maps of the average maximum acceleration and the coefficient of variation COV (COV=100(standard deviation)/average) displayed in Figure 4.15. The largest predicted PGA values (0.4-0.5 g) are observed in the coastal area north of the city of Catania. This effect is explained by a dominant effect of source directivity which is controlled by the fault geometry and receivers locations. Obviously the interpretation of PGA map has to be done considering the COV map too. Regions characterized by relatively high COV values suggest that PGA values can vary strongly depending on the way the fracture nucleates and develops during the rupture. The highest COV values are observed at receivers located along the coast in correspondence to the middle portion of the whole fault system. Due to the dominant effect of source directivity, the COV values are smaller for receivers located north of Catania.

The synthetic attenuation curves (PGA vs. minimum distance from the fault projection at the surface) show the expected variability with azimuth, controlled by the fault geometry and directivity (Fig. 4.16).

Assuming that our simulation data set is a representative sample of the possible rupture time histories, the 1 σ intervals shown in Figure 4.16 give an estimate of the expected PGA ranges. The computed curves are compared with the empirical ones obtained by Sabetta and Pugliese (1987) in the range of magnitude M=6-7 by regression analysis of the Italian strong motion database. Comparing the simulation results with the empirical relatinships, we distinguish profile directions for which there is a complete intersection with the predicted PGA range (45°, 135°, 165°, 180°), profiles with a weak intersection (15°, 30°, 60°, 105°, 120°) and profiles with no intersection at all (75°, 90°). The curves displayed in Figure 4.16 clearly show an azimuthal variation which is not taken into account by the Sabetta end Pugliese's empirical curves (1987).

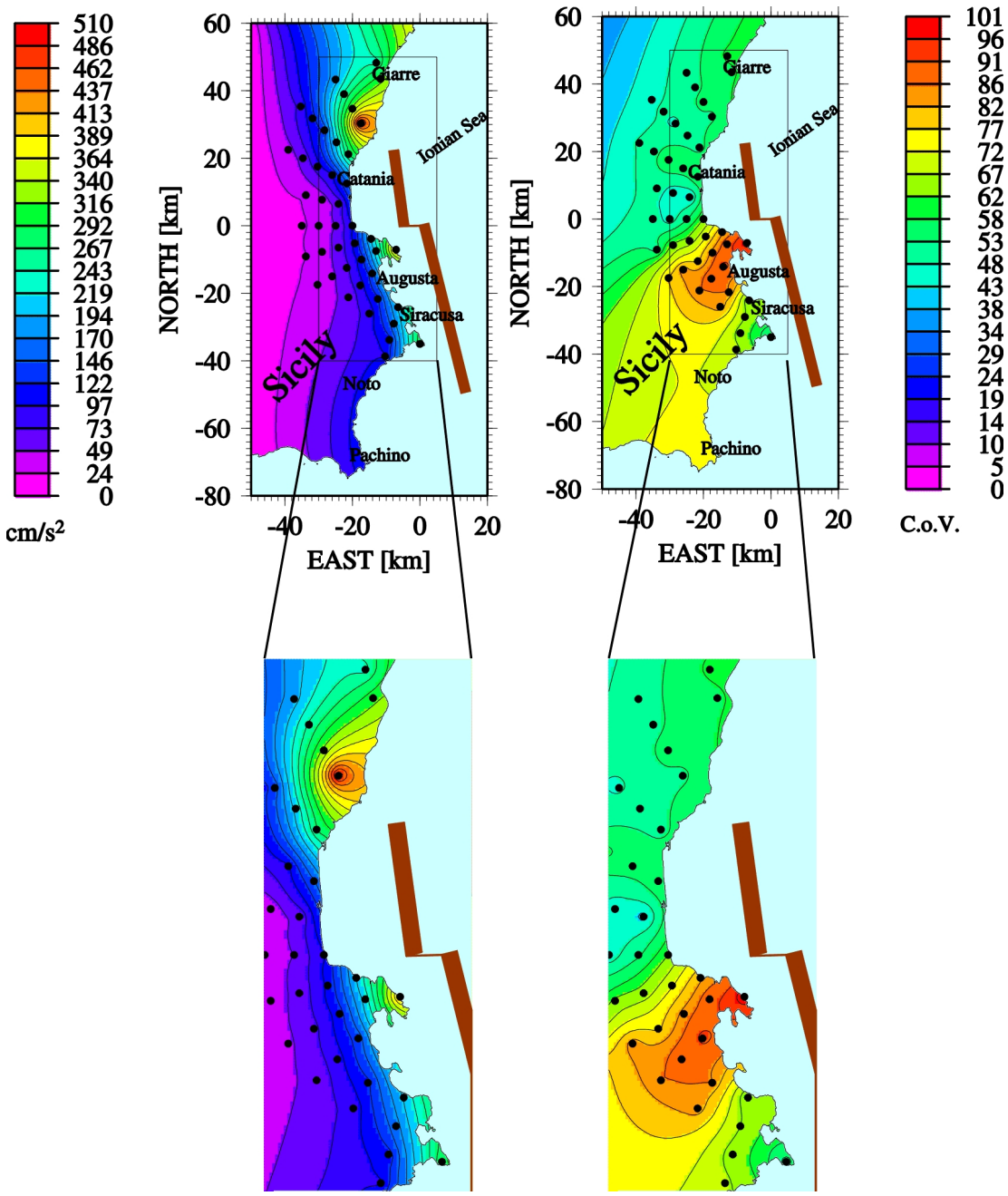

Figure 4.15 - Top-left. Map of simulated peak ground acceleration PGA (mean values on 100 simulations). Top-right. Map of coefficient of variation COV (see text for its definition). Bottom. Zoom of the area in the rectangles sketched in the upper figures. The brown thick lines in the figures represent the surface projection of the fault segments while the black circles represent the receivers locations.

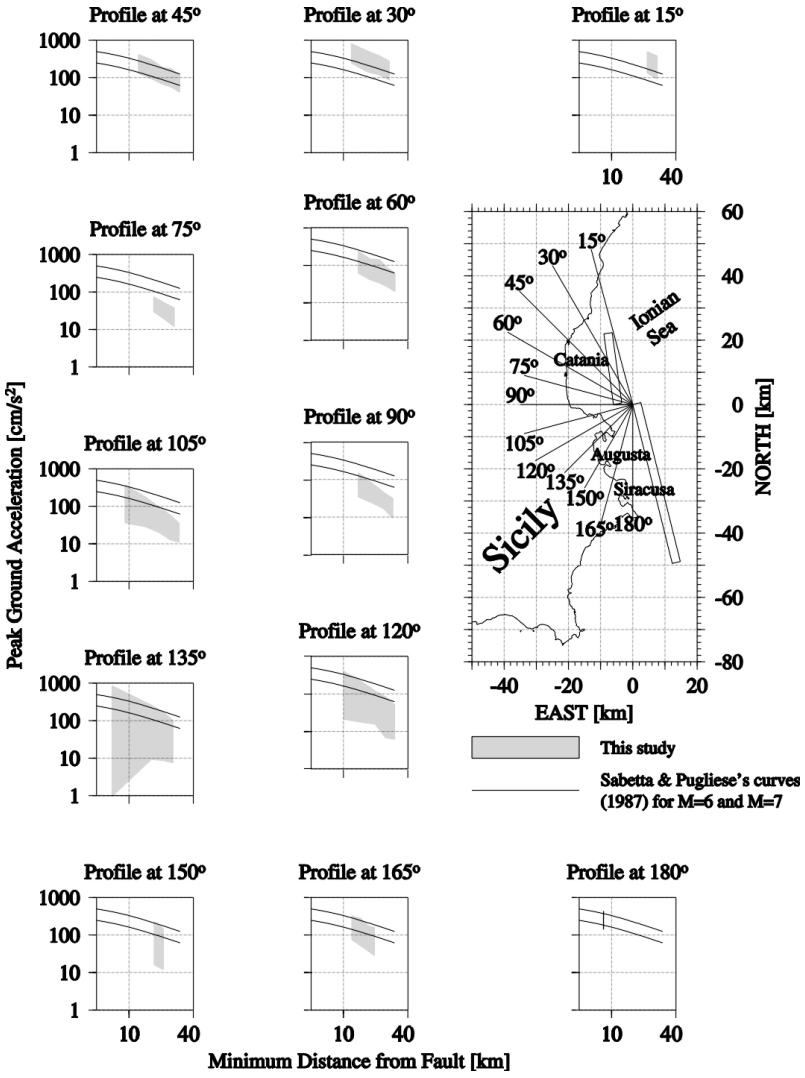

Figure 4.16 - Log/log plots of PGA (mean values and standard deviations) versus the minimum distance from the fault segments computed at different azimuths. The shaded zone corresponds to the 1σ variation interval. The figures also report the empirical curves (continous line) for M=6 and M=7 earthquakes obtained by Sabetta and Pugliese (1987).

4.4.3 *Results: simulation at urban scale*

As explained above, we computed the accelerograms in the urban area of Catania including the 1D transfer function computed by the Thomson-Haskell matrix method (Haskell, 1962) at several sites located on 4 geotechnical profiles constructed using borehole data and results of *in situ* and laboratory geotechnical tests (Faccioli, 1997).

Figure 4.17 shows the normalized pseudo-acceleration response spectra, computed using the Beck and Dowling (1988) algorithm, for four sites which are representative of the Catania subsoil. Significative amplification effects in the 5-20 Hz frequency range and attenuation at lower frequencies are observed at sites characterized by soft clay, scoriaceous lava flows and fill. These are 8 to 11 m thick and cover massive lava flows (site 1033) or consolitated blue clay (site 85). On the other hand, we observe a general high frequency attenuation effect in sites where Mt. Etna's massive lava flows, about 10 m thick, outcrop (site 365). South of Catania, recent alluvial deposits, with a thickness of some tens of meters (site 1268), produce small amplification effects in the 2-3 Hz and 5-10 Hz frequency bands.

Due to the high frequency amplification effects, we find an overestimation of a factor up to almost 2 for the normalized pseudo acceleration values in comparison with the Eurocode 8 curve for rock/stiff ground conditions. However this short period discrepancy, associated with the source complexity, can also be seen for the bedrock spectrum.

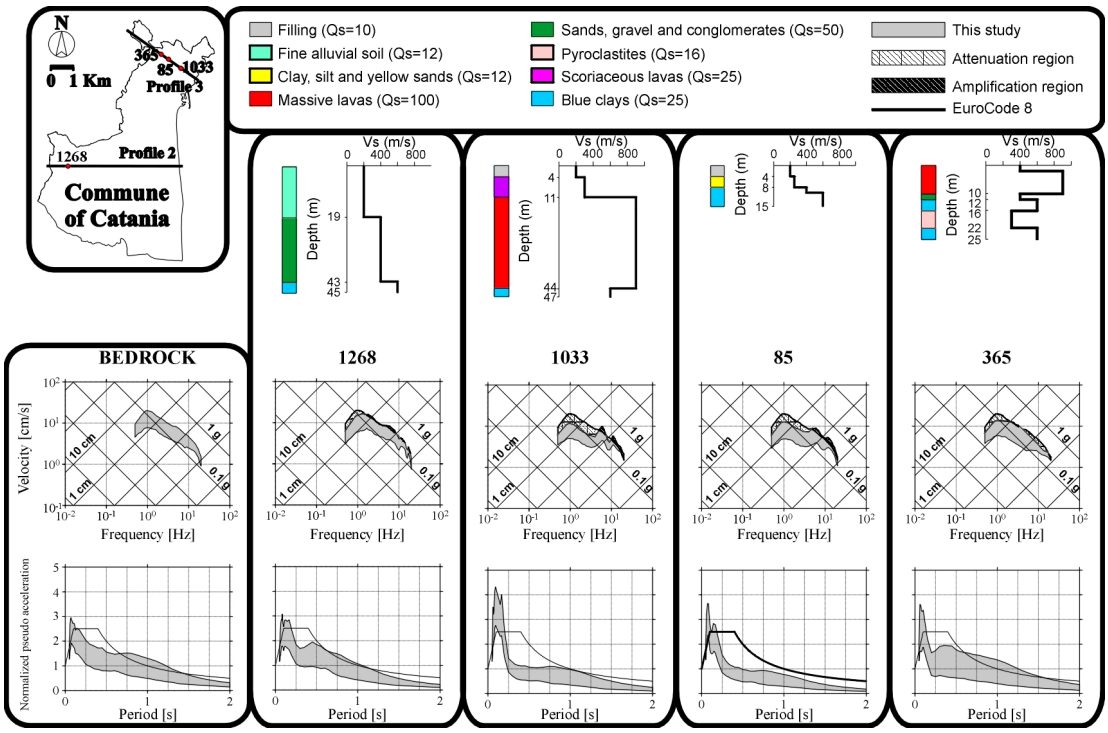

Figure 4.17 - Estimate of local site effect in Catania. Top. The 1D geologial characteristics and the shear wave velocity model for the sites considered in this study. Their locations are shown in the frame on the top left corner. Middle. Pseudo velocity response spectra. The shaded area corresponds to the 1 σ interval. Regions of attenuation and amplification with respect to the bedrock pseudo velocity response spectrum are also shown. Bottom. Normalized pseudo acceleration spectra. The shaded area corresponds to the 1 σ interval. For comparison, the Eurocode 8 spectrum (continous line) for rock/stiff ground is also illustrated.

References

Aki K. (1987). Strong motion seismology, in *Strong ground motion seismology (M. Erdik and M. Toksöz eds.)*, NATO ASI Series, Series C: Mathematical and Physical Sciences, D. Reidel Publishing Company, Dordrecht, **204**, 3-39

Aki K., Richards P.G. (1980). Quantitative seismology, theory and methods, *W.H. Freeman and Co.*, *San Francisco*, *USA*, **1** and **2**, 932 pp.

Amato A., Azzaro R., Basili A., Chiarabba C., Cocco M., Di Bona M., Selvaggi G. (1995). Main shock and aftershocks of the December 13, 1990, Eastern Sicily earthquake, *Annali di Geofisica*, **38**, 255-266

Beck J.L., Dowling M.J. (1988). Quick algorithms for computing either displacement, velocity or acceleration of an oscillator, *Earth. Eng. Struct. Dyn.*, **16**, 245-253

Bernard P., Madariaga R. (1984). A new asymptotic method for the modeling of near-field accelerograms, *Bull. Seism. Soc. Am.*, **74**, 539-557

Costa G., Panza G.F., Suhadolc P., Vaccari, F. (1993). Zoning of the Italian territory in terms of expected peak ground acceleration derived from complete synthetic seismograms, *J. Appl. Geophys*., **30**, 149-160

Decanini L., Mollaioli F., Panza G. F., Romanelli F. (1999). The realistic definition of the seismic input: an application to the Catania area. In: *Proc. Of Eres 1999* (G. Oliveto and C.A. Brebbia eds), Catania (Italy), 425-434, WIT Press, Boston.

Di Bona M., Cocco M., Rovelli A., Berardi R., Boschi E. (1995). Analysis of strong-motion data of the 1990 Eastern Sicily earthquake, *Annali di Geofisica*, **38**, 283-300

Emolo A., Zollo A. (1999). Accelerometric radiation simulation for the September 26, 1997 Umbria-Marche (Central Italy) mainshocks, submitted to *Bull. Seism. Soc. Am.*

Faccioli E. (coordinator) (1997). Geotechnical earthquake engineering characterization of the Catania municipal area, Technical report and CD-Rom prepared by *Ingegneria Geotecnica* for *CNR - Gruppo Nazionale Difesa Terremoti*, Milan, Italy (in Italian)

Farra V., Bernard P., Madariaga R. (1986). Fast near source evaluation of strong ground motion for complex source models, *Earth Source Mech. Geoph. Monograph*, *A.G.U.*, **37**, 121-130

Giardini D., Palombo B., Pino N. A. (1995). Long period modelling of MEDNET waveforms for the December 13, 1990 Eastern Sicily earthquake, *Annali di Geofisica*, **38**, 267-282.

Gusev A.A. (1983). Descriptive statistical model of earthquake source radiation and its application to an estimation of short period strong motion, *Geophys. J. R. Astron. Soc.* **74**, 787-800

Hanks T.C., Kanamori H. (1979). A moment-magnitude scale, *J. Geophys. Res.*, **84**, 2348-2352

Haskell N.A. (1953). The dispersion of surface waves in multilayered media, *Bull. Seism. Soc. Am.*, **43**, 17-34

Haskell N.A. (1962). Crustal reflection of plane SH waves, *J. Geophys. Res.*, **65**, 4751-4767

Herrero A., Bernard P. (1994). A kinematic self-similar rupture process for earthquakes, *Bull. Seism. Soc. Am.*, **84**, 1216-1229

Lachet C., Bard P.-Y. (1994). Numerical and theoretical investigations on the possibilities and limitations of Nakamura's technique, *J. Phys. Earth*, **42**, 377-397

Nakamura Y. (1989). A method for dynamic characteristics estimation of subsurface using microtremor on the ground surface. *QR Railway Tech. Res. Inst.,* **30**, 1.

Panza G.F. (1985). Synthetic seismograms: the rayleigh waves modal summation, *J. Geophys.* **58**, 125-145

Panza G.F., Romanelli F., Yanovskaya T. (1999). Synthetic Tsunami mareograms for realistic oceanic models, *Geophys. Journal Int.*, in press

Priolo E. (1999). 2-D spectral element simulations of destructive ground shaking in Catania (Italy), *J. Seism.*, **3**, 289-309

Priolo, E., and Michelini, A., (1999). Misure di rumore sismico ambientale nel Comune di Catania. With the collaboration of E. Faccioli, R. Addìa, A. Puglia, M. Mucciarelli, and R. Gallipoli. Progetto Catania. CNR-GNDT. U. O. OGS-Trieste. Rel. I-OGS/5/GDL/12/99, dd. 4.6.1999 (In Italian).

Romanelli F., Bing Z., Vaccari F., Panza G.F. (1996). Analytical computation of reflection and transmission coupling coefficients for Love waves, *Geophys. J. Int.*, **125**, 132-138

Romanelli F., Vaccari F. (1999). Site response estimation and ground motion spectral scenario in the Catania Area, *J. Seism.*, **3**, 311-326

Sabetta F., Pugliese A. (1987). Attenuation of peak horizontal acceleration and velocity from italian strong motion records, *Bull. Seism. Soc. Am.*, **77**, 1491-1513

Sommerville, P., Irikura, K., Graves, R., Sawada, S., Wald, D., Abrahamson, N., Iwasaki, Y., Kagawa, T., Smith, N., Kowada A. (1999). Characterizing crustal earthquake slip models for the prediction of strong ground motion, *Seim. Res. Lett.*, **70**, 59-80

Vaccari F., Gregersen S., Furlan M., Panza G.F. (1989). Synthetic seismograms in laterally heterogeneous, anelastic media by modal summation of P-SV waves, *Geophys. J. Int.*, **99**, 285-295

Wang, H., Nisimura A. (1999). On the behavior of near-source strong ground motion from the seismic records in down-hole array at Hyogoken-Nanbu earthquake, in *Earthquake Resistant Engineering Structures II (G. Oliveto and C. A. Brebbia eds)*, pp. 363-372, WIT Press, Southampton

Zollo A., Bobbio A., Emolo A., Herrero A., De Natale G. (1997). Modelling of ground acceleration in the near source range: the case of 1976 Friuli earthquake (M=6.5) Northern Italy, *J. Seism.*, **1**, 305-319